

Synthesis and Characterization of the Thiogermanic Acids $\text{H}_4\text{Ge}_4\text{S}_{10}$ and $\text{H}_2\text{Ge}_4\text{S}_9$

Steven A. Poling, Carly R. Nelson, Jacob T. Sutherland, and Steve W. Martin*

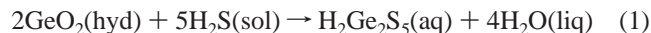
Department of Materials Science and Engineering, Iowa State University, Ames, Iowa 50011

Received: October 25, 2002; In Final Form: December 23, 2002

The synthesis and structure of the thiogermanic acids $\text{H}_4\text{Ge}_4\text{S}_{10}$ and $\text{H}_2\text{Ge}_4\text{S}_9$ are reported. A novel preparation method consisting of reacting germanium oxide with liquid hydrogen sulfide containing a trace amount of water is used to form $\text{Ge}_4\text{S}_{10}^{4-}$ ions. Evaporating the hydrogen sulfide solution at room temperature leaves an unstable $\text{H}_4\text{Ge}_4\text{S}_{10} \cdot x\text{H}_2\text{O}$ product. The stoichiometry and structure of the thermally stable anhydrous phase are dependent on reaction time. An $\text{H}_4\text{Ge}_4\text{S}_{10}$ product with an adamantane-like cage structure is obtained at shorter reaction times. Longer reaction times produce an $\text{H}_2\text{Ge}_4\text{S}_9$ product with a more complex cage unit, a higher symmetry unit cell, and increased thermal stability. Raman, infrared, powder X-ray diffraction, and thermogravimetric data are reported for both structures.

1. Introduction

Current and past efforts to produce protonated germanium sulfide complexes using hydrogen sulfide have resulted in the stoichiometric compound $\text{H}_4\text{Ge}_4\text{S}_{10}$. The existence of a $\text{Ge}_4\text{S}_{10}^{4-}$ unit cage was first reported as a $\text{Ge}_2\text{S}_5^{2-}$ ion in solution.¹ The reported $\text{H}_2\text{Ge}_2\text{S}_5$ thio-acid was synthesized by reacting a hydrous form of GeO_2 in an ethyl alcohol solution saturated with H_2S . The reaction was written as



Structural data were not reported for the reaction product $\text{H}_2\text{Ge}_2\text{S}_5$, it was simply noted to be a white amorphous solid. It was also reported to decompose slowly at 0 °C and was extremely soluble in water. This synthesis route proved to be inadequate for obtaining very pure samples without oxide contamination.

In the present study, a reaction medium consisting of liquid H_2S with a trace amount of water is implemented at room temperature. Under these conditions, it is possible to produce $\text{Ge}_4\text{S}_{10}^{4-}$ ions starting from quartz-type GeO_2 or glassy GeS_2 . This new preparation method is simple and functional, producing a structural evolution of the $\text{Ge}_4\text{S}_{10}^{4-}$ cage unit over time. In this article, the stoichiometry and structure of the resulting thiogermanic acid starting from GeO_2 as a precursor are characterized as functions of the reaction time.

There have been two reported structural isomers for the $\text{Ge}_4\text{S}_{10}^{4-}$ complex: adamantane and “double-decker.” Figure 1 shows the structures of the adamantane and double-decker $\text{Ge}_4\text{S}_{10}^{4-}$ complex anions. An adamantane-like unit was recently determined for the $\text{H}_4\text{Ge}_4\text{S}_{10}$ phase.² Adamantane units have also been determined for the phases of $\text{M}_4\text{Ge}_4\text{S}_{10}$ ($\text{M} = \text{Na}, \text{K}, \text{Rb}, \text{Cs}, \text{and Tl}$)^{3–6} and $\text{Ba}_2\text{Ge}_4\text{S}_{10}$.⁷ The adamantane unit is composed of four corner-shared GeS_4^{4-} tetrahedra. This structural unit was reported to be synthesized from solid-state reactions in evacuated silica tubes. Aqueous solution reactions were also reported for $\text{Cs}_4\text{Ge}_4\text{S}_{10} \cdot 3\text{H}_2\text{O}$, which was synthesized by adding GeS_2 to a concentrated aqueous solution of Cs_2S

where upon crystallization of the adduct was observed on standing.⁸ These units are usually highly symmetric with point symmetry group of T_d .⁹ Hence, the vibrational modes of the adamantane $\text{Ge}_4\text{S}_{10}^{4-}$ unit are distributed among the following Raman (R) and infrared (IR) fundamental vibrations: $\Gamma(T_d) = 3A_1(\text{R}) + 3E(\text{R}) + 3F_1(\text{inactive}) + 6F_2(\text{IR}, \text{R})$. A triclinic unit cell with space group $P\bar{1}$ is observed for the adamantane $\text{H}_4\text{Ge}_4\text{S}_{10}$ phase.² Orthorhombic and monoclinic crystal systems with space groups $Cmcm$, $C2/c$, and $C12/c1$ have been revealed for the $\text{M}_4\text{Ge}_4\text{S}_{10}$ adamantane compounds.^{4–6,10} A cubic unit cell with space group $Fd\bar{3}$ or $Fd\bar{3}m$ has been reported for $\text{Ba}_2\text{Ge}_4\text{S}_{10}$.⁷

Although germanium oxide-based complexes are known to form higher homologous structures, the only additional reported structure for $\text{Ge}_4\text{S}_{10}^{4-}$ based complexes is the double-decker.¹¹ This isomer has been previously reported for organo-substituted germanium sesquisulfides, $\text{R}_4\text{Ge}_4\text{S}_6$, where R represents an organic group.^{11,12} From a ring-strain perspective, the double-decker isomer is less favorable, having two sets of edge-shared tetrahedral units linked together. Structural solutions from X-ray diffraction (XRD) of $\text{R}_4\text{Ge}_4\text{S}_6$ indicate S–S distances in the shared edges of 3.30 Å,¹² which is less than the sum of the van der Waals radii of 3.60 Å. Additionally, ⁷⁷Se NMR distinguishes two distinct selenium environments for $\text{R}_4\text{Ge}_4\text{Se}_6$ and $\text{R}_4\text{Si}_4\text{Se}_6$ double-decker complexes.¹² The double-decker $\text{Ge}_4\text{S}_{10}^{4-}$ unit has a point symmetry group of D_{2h} ¹¹ and the vibrational modes are distributed among the following fundamental vibrations: $\Gamma(D_{2h}) = 7A_g(\text{R}) + 3A_u(\text{inactive}) + 5B_{1g}(\text{R}) + 4B_{1u}(\text{IR}) + 3B_{2g}(\text{R}) + 5B_{2u}(\text{IR}) + 3B_{3g}(\text{R}) + 6B_{3u}(\text{IR})$. Cubic and monoclinic crystal systems with space groups $I23$ and $C2/c$, respectively, have been revealed for the organo-substituted $\text{R}_4\text{Ge}_4\text{S}_6$ double-decker compounds.^{11,12}

2. Experimental Section

2.1. Sample Preparation. A typical reaction consisted of placing 500 mg (± 1 mg) of commercial quartz-type GeO_2 powder (Cerac 99.999%, ~ 325 mesh) in an alumina tube, which in turn was placed inside a type 316 stainless steel reaction vessel. The total free volume inside the reaction vessel was ~ 72 mL. The reactor was sealed with a Teflon O-ring gasket and a Swagelok type 316 stainless steel needle valve. The assembled

* Corresponding author. E-mail: swmartin@iastate.edu. Phone: (515) 294–0745.

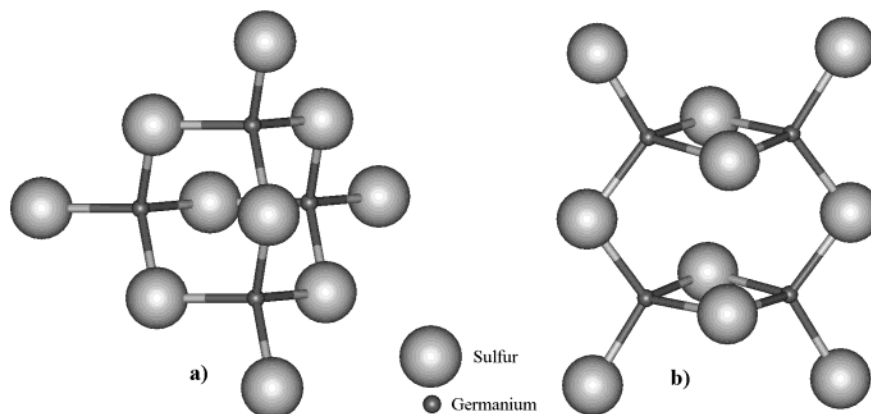


Figure 1. (a) Ball-and-stick schematic of an adamantane $\text{Ge}_4\text{S}_{10}^{4-}$ structural unit. Cations of H, Na, K, Rb, Cs, Tl, and Ba have been shown to form these units with GeS_2 . (b) Ball-and-stick schematic of a double-decker $\text{Ge}_4\text{S}_{10}^{4-}$ structural unit. Organo-substituted GeS_2 compounds have been shown to form these units.

reactor was evacuated to ~ 75 mTorr, cooled with liquid nitrogen ($T < -86^\circ\text{C}$), and back-filled with ~ 7 g of H_2S gas (Matheson, 99.9 mol %). For these experiments, the reaction rate was dependent on the impurity water content found in the commercial purity H_2S gas cylinder (~ 0.02 mol %). The reactions took place at room temperature ($\sim 22^\circ\text{C}$) where liquid H_2S was present in the reactor under its own vapor pressure (~ 267 psia). The total reaction time was varied from 1 to 8 weeks. Reaction times may be decreased by the further addition of a small amount of water (e.g. ~ 1 mol % of H_2O to H_2S) to the impurity water content of the H_2S . After the designated reaction time, the resulting H_2S – H_2O solution inside the reactor was evaporated through a NH_4OH solution. The reactor was then opened inside a glovebox with low oxygen and water content (< 5 ppm), where mass measurements of the resulting product were recorded as a function of time. Intercalated H_2O may take up to a day to fully dissipate; heating may be used to speed this process.

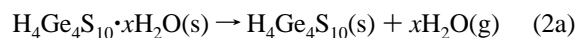
2.2. Spectroscopic Measurements. Structural investigations were conducted using Raman scattering, infrared absorption, and powder XRD. Raman spectra were obtained using a Bruker FT-Raman RFS 100/S spectrometer with a 1064-nm Nd:YAG laser using 2 cm^{-1} resolution and 300 mW of power focused on ~ 0.1 mm diameter spot size. Powdered samples were packed into an aluminum sample holder and covered with amorphous tape. Infrared absorption spectra were obtained using a Bio-Rad FTS-40 mid-infrared (mid-IR) spectrometer and a Bio-Rad FTS-60V far-infrared (far-IR) spectrometer using 4 cm^{-1} resolution. Pressed KBr powder pellets were prepared using ~ 3 wt % of sample for mid-IR, and powder mixed with Nujol sandwiched between two high-density polyethylene sheets was used for the far-IR. Powder XRD spectra were collected from 3° to 70° 2θ using a Seimens D500 diffractometer with $\text{Cu K}\alpha$ radiation ($\lambda = 1.54178\text{ \AA}$). Powdered samples were packed into a polycarbonate sample disk with no amorphous cover. Care was taken to minimize atmospheric exposure; after 1 h scan time no structural changes were observed.

2.3. Thermal Measurements. Thermal investigations were performed using a Perkin-Elmer Thermogravimetric Analyzer TGA 7 (TGA). A 20 mL/min flow of N_2 was used as the sample purge to prevent any oxidation reactions. About 25 mg of each sample was placed inside an aluminum sample pan. A heating rate of $10^\circ\text{C}/\text{min}$ was used for all TGA experiments.

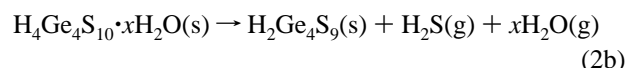
3. Results and Discussion

3.1. Mass Change. Sample masses were recorded for all reactions as a function of reaction time. There was minimal

reaction for the first week at room temperature: e.g., ~ 2 wt % increase. This mass increase was most likely due to hydroxyl group formation in the GeO_2 as can be seen in the mid-IR spectra in Figure 3; the initial H_2O contamination was accredited to the commercial purity H_2S gas. Hydroxyl group formation is also in agreement with the observation that hydrated GeO_2 was necessary for the reaction to proceed.¹ A white-to-beige colored product was collected for reaction times longer than 1 week. Two-week reactions produced stabilized sample masses consistent with ~ 92 wt % $\text{H}_4\text{Ge}_4\text{S}_{10}$ with the balance as GeO_2 ; this is in agreement with the mid-IR spectra in Figure 3. Stabilized masses from 3- and 4-week reaction times suggest mixed-phase products, whereas 8-week reactions indicated an $\text{H}_2\text{Ge}_4\text{S}_9$ phase. As an example, a complete conversion to the stoichiometric compound $\text{H}_2\text{Ge}_4\text{S}_9$ from 500 ± 1 mg of GeO_2 would yield 694 ± 2 mg of product. A mixed oxy-sulfide phase of $\text{H}_4\text{Ge}_4\text{S}_8\text{O}_2$ would yield a similar mass, but no evidence for this type of phase is present in the corresponding vibrational spectra. Immediately after opening the reactors, the recorded sample masses were much higher. This is consistent with hydrous $\text{H}_4\text{Ge}_4\text{S}_{10} \cdot x\text{H}_2\text{O}$ phases stabilized by the cooler temperature resulting from endothermic boiling-off of H_2S during rapid removal. For the 2- and 8-week reaction products, the decomposition reaction upon warming to room temperature may be written as



and



respectively. About 1 day after removing the liquid H_2S , all intercalated H_2O was evaporated and the decomposition reaction was complete.

3.2. Raman Scattering. Figure 2 presents the unpolarized Raman spectra of the stabilized products as a function of reaction time in liquid H_2S at room temperature. The vibrational frequencies in the spectra are time independent after opening the reactor; for reaction times greater than one week, this implies the $\text{Ge}_4\text{S}_{10}^{4-}$ structural cage unit is present in both the hydrous and anhydrous phases. For 1 week of reaction time, the vibrational bands assigned to quartz-type GeO_2 are still present and the strongest band located at $\sim 443\text{ cm}^{-1}$ can be assigned to Ge–O–Ge symmetric stretching.¹³ For 2 weeks of reaction time, new vibrational bands appear, suggesting a structure that is consistent with adamantane-like $\text{Ge}_4\text{S}_{10}^{4-}$ units. Table 1

TABLE 1: Raman and IR Mode Assignments for the 2-Week Reaction Product $\text{H}_4\text{Ge}_4\text{S}_{10}$ ^a

	$\text{H}_4\text{Ge}_4\text{S}_{10}$ and $\text{H}_4\text{Ge}_4\text{S}_{10} \cdot x\text{H}_2\text{O}$ adamantane		$\text{Cs}_4\text{Ge}_4\text{S}_{10}$ adamantane ⁹		$\text{Na}_4\text{Ge}_4\text{S}_{10}$ adamantane ³	lithium dithiogermante glass ²¹	silver dithiogermanate glass ¹⁸	
	Raman	IR	Raman	IR	Raman	Raman	Raman	IR
$\nu_{15}(\text{F}_2)$	107		116	121				
$\nu_{14}(\text{F}_2)$	145		144	148				
$\nu_3(\text{A}_1)$	187		193		200			
$\nu_2(\text{A}_1) \{ \nu_s(\text{Ge}-\text{S}-\text{Ge}) \}$	355		340		354	350	339	330
$\nu_1(\text{A}_1) \{ \nu_s(\text{Ge}-\text{S}^-) \}$	407, 416	414	462		470	425	415	412
$\nu(\text{S}-\text{H})$	2484, 2515	2479, 2511						

^a T_d point group symmetry is assumed for the adamantane $\text{Ge}_4\text{S}_{10}^{4-}$ unit cage. Assignments for comparable reference systems are also presented. All units are in wavenumbers (cm^{-1}).

TABLE 2: Raman and IR Mode Assignments for the 8-Week Reaction Product $\text{H}_2\text{Ge}_4\text{S}_9$ ^a

	$\text{H}_2\text{Ge}_4\text{S}_9$ and $\text{H}_4\text{Ge}_4\text{S}_{10} \cdot x\text{H}_2\text{O}$		Glassy GeS_2		High Temp 2D phase ($\beta\text{-GeS}_2$)		Low Temp 3D phase ($\alpha\text{-GeS}_2$)	
	Raman	IR	Raman	IR	Raman	IR	Raman	IR
bond-bending	106, 127, 152, 172, 197, 240		105 ¹⁹ , 112 ¹⁶ , 110, 150 ¹⁸	149 ¹⁹ , 147 ¹⁶ , 115, 153 ¹⁸				
A_1 corner-shared $\{ \nu_s(\text{Ge}-\text{S}-\text{Ge}) \}$	344	338	342 ^{18,14,19} , 343 ¹⁶	328 ¹⁹ , 340 ^{18,16}	356 ¹⁵ , 361 ²⁰ , 363 ²²	342 ²⁰	339 ¹⁵ , 342 ²⁰	332 ²⁰
A_1 edge-shared $\{ \nu_s(\text{Ge}-\text{S}-\text{Ge}) \}$	352		374 ^{b,14} , 370 ^{b,16}	372 ¹⁶	363 ¹⁵ , 383 ²²			
F_2 $\{ \nu_{as}(\text{Ge}-\text{S}-\text{Ge}) \}$	363	370	375 ¹⁹ , 390 ¹⁶ , 368 ¹⁸	367 ¹⁹ , 395 ¹⁶ , 377 ¹⁸	340–450, exc. A_1 ²⁰	350–450 ²⁰	340–450, exc. A_1 ²⁰	350–450 ²⁰
bond-stretching	380	386		409 ¹⁹				
A_1 and high F_2	401 409 435 445	403 411 434 448						
$\nu(\text{S}-\text{H})$	2520	2517		2525 ²³				

^a Local T_d point group symmetry is assumed for isolated GeS_4^{4-} units. Assignments for comparable reference systems are also presented. All units are in wavenumbers (cm^{-1}). ^b Although controversial, in glassy GeS_2 the A_1 companion band is often attributed to edge shared tetrahedral units.

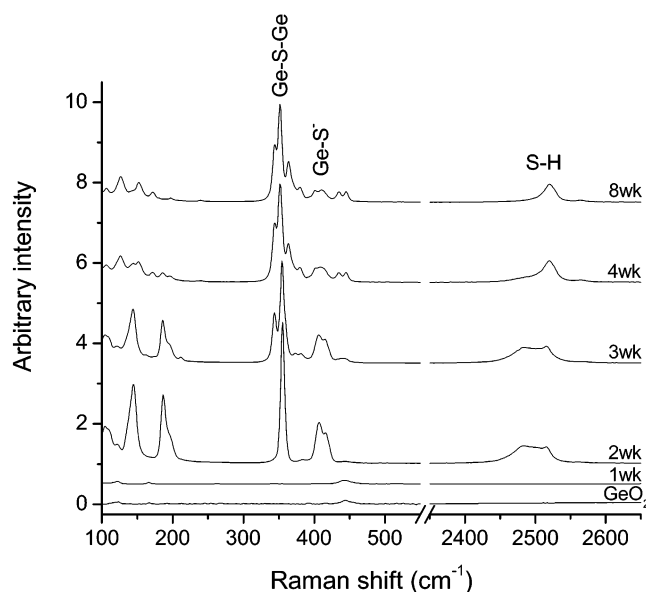


Figure 2. Raman spectra of GeO_2 reacted with liquid H_2S at room temperature as a function of time. No reaction is noted for 1 week; 2-week reaction time produces a highly vibrational symmetric adamantane $\text{H}_4\text{Ge}_4\text{S}_{10}$ phase; 3- and 4-week reaction times produce mixed phases, whereas 8 weeks of reaction time appears to produce an $\text{H}_2\text{Ge}_4\text{S}_9$ phase with a more complex cage unit.

presents select Raman and IR vibrational mode assignments for the adamantane $\text{H}_4\text{Ge}_4\text{S}_{10}$ phase and representative reference systems assuming T_d point group symmetry. In a polarized Raman spectrum, the strongest bands may be assigned to the 3A_1 vibrations for the adamantane structural unit.⁹ In the

unpolarized spectrum obtained for 2 weeks of reaction time, the strongest intensity band observed at $\sim 355 \text{ cm}^{-1}$ is assigned to $\text{Ge}-\text{S}-\text{Ge}$ symmetrical bridge-stretching mode $\nu_2(\text{A}_1)$. This value is within resolution for that reported for $\text{Na}_4\text{Ge}_4\text{S}_{10}$.³ The band observed at $\sim 187 \text{ cm}^{-1}$ may be assigned to $\text{Ge}-\text{S}-\text{Ge}$ symmetrical bridge bending mode $\nu_3(\text{A}_1)$. The two overlapping bands centered around ~ 407 and $\sim 416 \text{ cm}^{-1}$ may be attributed to $\text{Ge}-\text{S}^-$ nonbridging or symmetrical terminal stretching mode $\nu_1(\text{A}_1)$. This is consistent with two broad bands with peak intensities located around ~ 2484 and $\sim 2515 \text{ cm}^{-1}$ assigned to $\text{S}-\text{H}$ bond stretching. Two distinct bands indicate two unique hydrogen environments for the $\text{H}_4\text{Ge}_4\text{S}_{10}$ phase.

The products associated with 3 and 4 weeks of reaction time suggest mixed phases, whereas the product from 8 weeks of reaction time indicates a different structure all together. Although it is not possible to fully resolve this new structure from the unpolarized Raman spectrum alone, inferences may be drawn from comparisons with established systems. Without knowing the structure, one may consider the individual GeS_4^{4-} units possessing T_d symmetry to suggest mode assignments using crystalline and glassy GeS_2 as references. Table 2 presents Raman and IR suggested vibrational mode assignments of the $\text{H}_2\text{Ge}_4\text{S}_9$ phase for 8 weeks of reaction time. In the spectrum, medium-intensity vibrational bands at ~ 106 , ~ 127 , ~ 152 , and $\sim 172 \text{ cm}^{-1}$ and weak-intensity bands at ~ 197 and $\sim 240 \text{ cm}^{-1}$ are located in the frequency region consistent with translational, rotational, and bond-bending E and lower frequency F_2 modes.^{14–16} The strongest bands with peak intensity values at ~ 344 , ~ 352 , and $\sim 363 \text{ cm}^{-1}$ may be attributed to $\text{Ge}-\text{S}-\text{Ge}$ stretching modes. Specifically, the bands at ~ 344 and $\sim 352 \text{ cm}^{-1}$ may be attributed to A_1 symmetric stretching due to weak

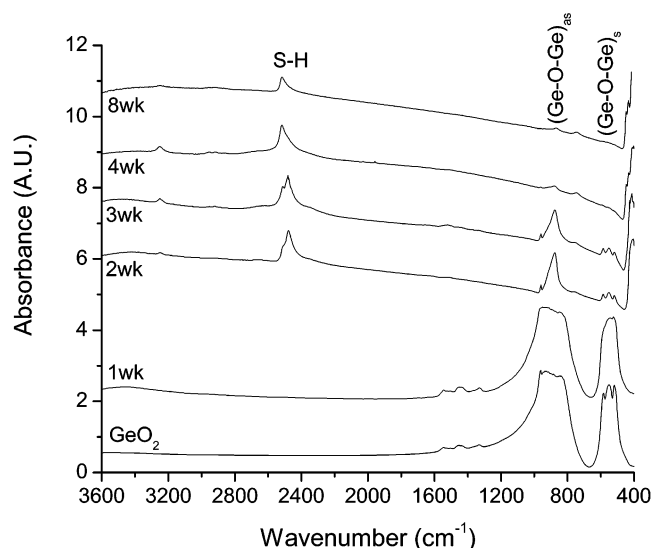


Figure 3. Mid-IR spectra of GeO_2 reacted with liquid H_2S at room temperature as a function of time. No reaction is noted for 1 week; 2-week reaction time produces an S–H stretching mode around 2500 cm^{-1} that becomes less IR active with increased reaction time. Vibrational modes associated with the starting GeO_2 reduce in intensity with increasing reaction time.

IR activity. In contrast, the band at $\sim 363\text{ cm}^{-1}$ may be attributed to F_2 asymmetric stretching due to strong IR activity. The ratio of the band intensities at ~ 344 and $\sim 352\text{ cm}^{-1}$ are roughly consistent with corner-shared and edge-shared tetrahedral units, respectively, associated within the double-decker isomer. Note, the $\sim 344\text{ cm}^{-1}$ band intensity was observed to increase after the mass of the reaction product stabilized, implying bridging of discrete units into rings and/or chains. The medium-intensity vibrational bands with peak intensities located at ~ 380 , ~ 401 , ~ 409 , ~ 435 , and $\sim 445\text{ cm}^{-1}$ may be generally attributed to A_1 terminal stretching mode and higher F_2 stretching modes.¹⁵ Specifically, the broad band located at $\sim 409\text{ cm}^{-1}$ is close to the Ge-S^- nonbridging mode for the 2-week reaction time. The S–H bond stretching mode for the 8-week reaction time has a strong intensity peak located $\sim 2520\text{ cm}^{-1}$; this peak is narrower in frequency and half the integrated area of the S–H stretching mode for the 2-week reaction. This indicates one unique hydrogen environment for the $\text{H}_2\text{Ge}_4\text{S}_9$ phase.

The Raman spectrum resulting from 8 weeks of reaction time is more consistent with an isomer having reduced vibrational symmetry and a more complex cage unit. Again, it is suggested that intact $\text{Ge}_4\text{S}_{10}^{4-}$ unit cages are linked together to form rings and/or chains. The possible formation of a double-decker isomer of $\text{Ge}_4\text{S}_{10}^{4-}$ units may be the result of extensive reaction time with hydrostatic pressure equal to that of the vapor pressure of H_2S at room temperature, i.e., 267 psia (1.8 MPa).

3.3 Infrared Spectra. Figure 3 presents the mid-IR spectra of the stabilized products as a function of reaction time in liquid H_2S at room temperature. For 1 week of reaction time, the resulting spectrum looks very similar to that of the starting GeO_2 compound. The broad bands located around ~ 877 and $\sim 553\text{ cm}^{-1}$ may be assigned to Ge-O-Ge asymmetric stretching modes ν_{as} ($860, 894, 989\text{ cm}^{-1}$) and Ge-O-Ge symmetric stretching modes ν_{s} ($464, 569\text{ cm}^{-1}$), respectively.¹⁷ Additionally, a weak O–H stretching mode centered around $\sim 3400\text{ cm}^{-1}$ is present and is consistent with the hydration process as the first step of the total reaction. For a reaction time of 2 weeks, the corresponding mid-IR spectrum shows a reduction in the intensity of Ge-O-Ge asymmetric stretching and symmetric stretching modes. Two overlapping S–H stretching modes

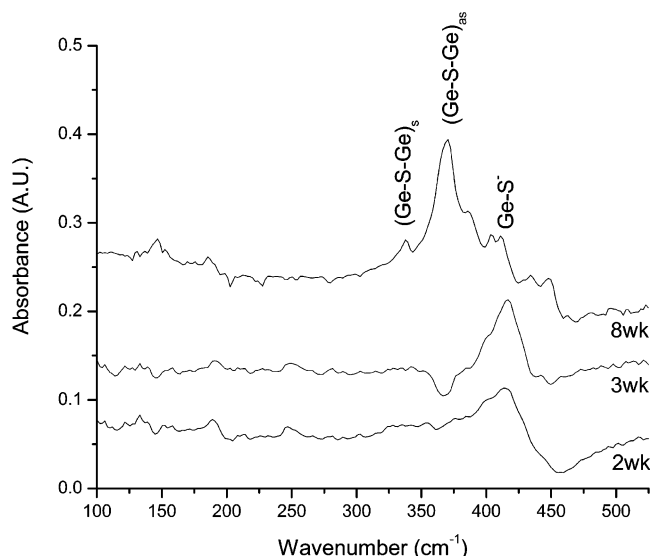


Figure 4. Far-IR spectra of GeO_2 reacted with liquid H_2S at room temperature as a function of time. Two and three-week reaction times produce IR active Ge-S^- terminal stretching modes at $\sim 414\text{ cm}^{-1}$. Eight-week reaction time produces additional IR active modes including the strong asymmetric stretching mode at $\sim 370\text{ cm}^{-1}$.

centered around ~ 2479 and $\sim 2511\text{ cm}^{-1}$ are also present. As noted from the corresponding Raman spectrum, the presence of two distinct bands indicates two unique hydrogen environments. For reaction times longer than 4 weeks, the Ge-O-Ge modes are almost completely absent. Additionally, the S–H stretching mode becomes less IR active, narrower in width, and located at a higher frequency with a peak intensity around $\sim 2517\text{ cm}^{-1}$. As with the corresponding Raman spectrum, this suggests only one unique hydrogen environment is present.

Figure 4 presents the far-IR spectra of stabilized products as a function of reaction time in liquid H_2S at room temperature. The products from 2 and 3 weeks of reaction time are less IR active compared with that from 8 weeks of reaction time. On the basis of the corresponding Raman spectrum, an adamantane structure having a point symmetry group of T_d is suggested for the 2-week reaction-time product. The band center at $\sim 414\text{ cm}^{-1}$ may be partially attributed to the Ge-S^- terminal stretching mode $\nu_1(\text{A}_1)$. Infrared activity of this mode indicates a reduction in local T_d symmetry to at least C_{3v} symmetry with a terminal bond to hydrogen.¹⁸ Additional asymmetric modes may also contribute to the broad feature in this frequency range, specifically $\nu_{11}(\text{F}_2)$ and $\nu_{10}(\text{F}_2)$ were reported at 395 and 455 cm^{-1} , respectively, for $\text{Cs}_4\text{Ge}_4\text{S}_{10}$.⁹ Bands were also observed for $\text{Na}_4\text{Ge}_4\text{S}_{10}$ at 390, 405, 420, 440, and 455 cm^{-1} .⁷

The far-IR spectrum of the 3-week reaction-time product contains the same gross features as the 2-week reaction-time product. The far-IR spectrum of the compound produced with 8 weeks of reaction time is notably different. As with the corresponding Raman spectrum interpretation, individual $\text{Ge}_4\text{S}_{10}^{4-}$ units possessing T_d symmetry may be considered. The dominant band with a peak intensity located at $\sim 370\text{ cm}^{-1}$ may be assigned to the F_2 asymmetric bridge stretching mode; the $\sim 7\text{ cm}^{-1}$ shift in frequency from that observed in Raman, $\sim 363\text{ cm}^{-1}$, may be the result of intermolecular coupling of tetrahedral units through bridging sulfur atoms.¹⁹ The weak peak observed at $\sim 338\text{ cm}^{-1}$ may be attributed to the A_1 symmetric bridge stretching mode. IR activity of this peak infers that perfect T_d point group symmetry is not present.²⁰ Vibrational bands located at ~ 386 , ~ 403 , ~ 411 , ~ 434 , and $\sim 448\text{ cm}^{-1}$ are in close agreement with those observed in the Raman spectrum. The

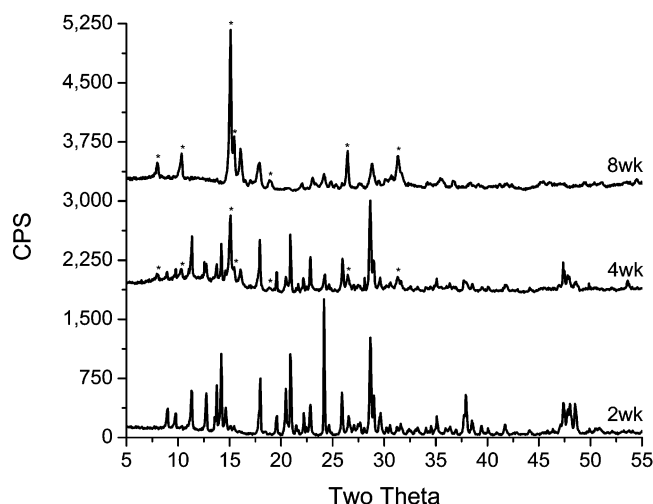


Figure 5. XRD spectra of GeO_2 reacted with liquid H_2S at room temperature as a function of time. Unique crystalline phases are realized for reaction times of 2 and 8 weeks; 4 weeks produces a mixed phase. Asterisks are drawn to aid the identification of the 8-week structure in the four 4-week mixed phase using distinguishable peaks.

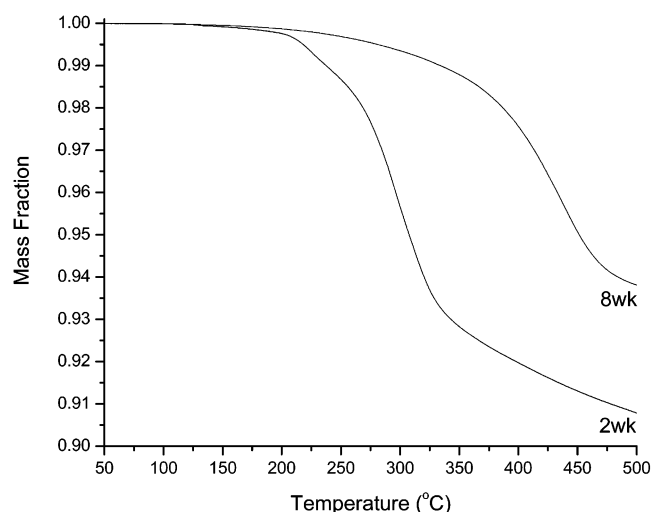


Figure 6. TGA spectra of GeO_2 reacted with liquid H_2S at room temperature as a function of time. A reaction time of 2 weeks produces a less thermally stable phase than that of 8 weeks. Theoretical decomposition from pure $\text{H}_4\text{Ge}_4\text{S}_{10}$ and $\text{H}_2\text{Ge}_4\text{S}_9$ thiogermanic acids to germanium disulfide is realized at 0.89 and 0.94 mass fractions, respectively.

location of these bands is again consistent with A_1 terminal stretching and higher F_2 stretching modes. The complex IR and Raman spectra suggest a more complex structural cage unit.

3.4. X-ray Diffraction. Figure 5 presents the raw powder XRD spectra of the stabilized products as a function of reaction time in liquid H_2S at room temperature. Peaks corresponding to the starting quartz-type GeO_2 were not readily identified in the resulting spectra. Unique phases were evident for the 2- and 8-week reaction times; the 4-week reaction time produced a mixed phase. The diffractogram for the 2-week reaction time product possesses peaks located at 8.97° and 9.76° 2θ , indicating crystal periodicity up to 9.858 \AA and 9.062 \AA , respectively. The diffractogram corresponding to 8 weeks of reaction time is notably simpler, suggesting a more symmetric unit cell. Low angle diffraction peaks are located at 8.01° and 10.35° 2θ , indicating crystal periodicity up to 11.038 \AA and 8.547 \AA , respectively. The growth of single crystals and XRD structural solutions are not yet performed for the product from 8 weeks

of reaction time; thus the existence of a double-decker complex isomer remains unresolved.

3.5. Thermal Analysis. Figure 6 presents the TGA spectra of the stabilized products of 2- and 8-week reaction times in liquid H_2S at room temperature. Decomposition onset temperatures corresponding to the 2-week reaction product $\text{H}_4\text{Ge}_4\text{S}_{10}$ and the 8-week reaction product $\text{H}_2\text{Ge}_4\text{S}_9$ were observed at $\sim 250^\circ\text{C}$ and $\sim 360^\circ\text{C}$, respectively. Theoretical decomposition of pure phases of $\text{H}_4\text{Ge}_4\text{S}_{10}$ and $\text{H}_2\text{Ge}_4\text{S}_9$ into GeS_2 would produce final mass fractions of 0.89 and 0.94, respectively. Thermal relaxation of the 8-week reaction product converting to the adamantane structural unit before decomposition was not observed in the corresponding Raman spectra; initial decomposition of both phases formed a glassy GeS_2 product. After decomposition at 500°C , the observed Raman spectra of both isomers exhibited a strong Ge—S—Ge symmetrical bridge stretching mode at $\sim 360 \text{ cm}^{-1}$; upon further heating ($\sim 700^\circ\text{C}$), this band grew in intensity producing Raman spectra which were consistent with that reported for the high temperature 2-D crystalline GeS_2 (denoted as $\beta\text{-GeS}_2$ in this article).¹⁵

4. Conclusions

Novel reactions of liquid H_2S with GeO_2 produce $\text{Ge}_4\text{S}_{10}^{4-}$ ions in solution. These reactions involve kinetic processes including hydroxide to hydrosulfide group transformation, adamantane cage formation, and cage restructuring. Evaporating the H_2O — H_2S solution leaves thermally unstable $\text{H}_4\text{Ge}_4\text{S}_{10} \cdot x\text{H}_2\text{O}$ units that decompose into the thermally stable anhydrous $\text{H}_4\text{Ge}_4\text{S}_{10}$ or $\text{H}_2\text{Ge}_4\text{S}_9$ phases. In general, the adamantane $\text{H}_4\text{Ge}_4\text{S}_{10}$ phase is obtained from shorter reaction times, whereas an $\text{H}_2\text{Ge}_4\text{S}_9$ phase with a more complex cage unit and a more symmetric unit cell is suggested for longer reaction times. The Raman, IR, and XRD structural evolution as a function of reaction time indicates a strongly kinetically controlled formation rate with presumably the hydrostatic pressure of liquid H_2S as the driving force. Ultimately, this $\text{H}_2\text{Ge}_4\text{S}_9$ phase realized from longer reaction times is approximately 110°C more thermally stable than that of the adamantane $\text{H}_4\text{Ge}_4\text{S}_{10}$ phase. For both thiogermanic acids, however, the thermal decomposition product is determined to be glassy GeS_2 from corresponding Raman spectra.

Acknowledgment. This material is based on the work funded by the United States Department of Energy's Hydrogen Program under Cooperative Agreement No. DE-FC36-00GO1-531. Chad Martindale is thanked for help in obtaining far-IR spectra.

References and Notes

- (1) Willard, H. H.; Zuehlke, C. W. The preparation and properties of potassium thiogermanate and thiogermanic acid; *J. Am. Chem. Soc.* **1943**, *65*, 1887–1889.
- (2) Poling, S. A.; Nelson, C. R.; Sutherland, J. T.; Martin, S. W., to be submitted.
- (3) Barrau, B.; Ribes, M.; Maurin, M.; Kone, A.; Souquet, J. L. Glass formation, structure and ionic conduction in the Na_2S — GeS_2 system; *J. Non-Cryst. Solids* **1980**, *37*, 1–14.
- (4) Klepp, K. O.; Fabian, F. New chalcogenogermanates with adamantane type complex anions: preparation and crystal structures of $\text{K}_4\text{Ge}_4\text{S}_{10}$; $\text{Rb}_4\text{Ge}_4\text{S}_{10}$; $\text{Rb}_4\text{Ge}_4\text{Se}_{10}$; and $\text{Cs}_4\text{Ge}_4\text{Se}_{10}$; *Z. Naturforsch., B: Chem. Sci.* **1999**, *54*, 1499–1504.
- (5) Klepp, K. O.; Zeitlinger, M. Crystal structure of tetracesium decasulfidotetragermanate, $\text{Cs}_4\text{Ge}_4\text{S}_{10}$; *Z. Kristallogr.* **2000**, *215*, 7–8.
- (6) Eulenberger, V. G. Die Kristallstruktur des Thallium(I)thiogermanats $\text{Tl}_4\text{Ge}_4\text{S}_{10}$; *Acta Crystallogr.* **1976**, *B32*, 3059–3063.

- (7) Ribes, M.; Olivier-Fourcade, J.; Philippot, E.; Maurin, M. Structural study of thio compounds with tetrane type anionic groups. Sodium thiosilicate ($\text{Na}_4\text{Si}_4\text{S}_{10}$), sodium thiogermanate ($\text{Na}_4\text{Ge}_4\text{S}_{10}$), and barium thiogermanate ($\text{Ba}_2\text{Ge}_4\text{S}_{10}$); *J. Solid State Chem.* **1973**, *8*, 195–205.
- (8) Pohl, V. S.; Krebs, B. Darstellung und Struktur von $\text{Cs}_4\text{Ge}_4\text{S}_{10} \cdot 3\text{H}_2\text{O}$; *Z. Anorg. Chem.* **1976**, *424*, 265–272.
- (9) Muller, A.; Cyvin, B. N.; Cyvin, S. J.; Pohl, S.; Krebs, B. Spectroscopic studies of As_4O_6 , Sb_4O_6 , $\text{P}_4\text{S}_{10}^{4-}$ and organometallic compounds containing the M_4X_6 cage. The Raman and IR spectrum of $\text{Ge}_4\text{S}_{10}^{4-}$; *Spectrochim. Acta* **1976**, *32A*, 67–74.
- (10) Philippot, E.; Ribes, M.; Lindqvist, O. Crystal structure of sodium germanium sulfide ($\text{Na}_4\text{Ge}_4\text{S}_{10}$); *Rev. Chim. Miner.* **1971**, *8*, 477–489.
- (11) Ando, W.; Kadowaki, T.; Kabe, Y.; Ishii, M. A Germanium Sesquisulfide, $(t\text{BuGe})_4\text{S}_6$, without Adamantane Structure; *Angew. Chem., Int. Ed. Engl.* **1992**, *31*, 59–61.
- (12) Unno, M.; Kawai, Y.; Shioyama, H.; Matsumoto, H. Synthesis, Structures, and Properties of Tricyclotetrasilachalcogenanes ($\text{Thex}_2\text{Si}_2\text{E}_2$)- E_2 ($\text{E} = \text{S}, \text{Se}$) and Tricyclotetragermachalcogenanes ($\text{Thex}_2\text{Ge}_2\text{E}_2$)- E_2 ($\text{E} = \text{S}, \text{Se}$); *Organometallics* **1997**, *16*, 4428–4434.
- (13) Mernagh, T. P.; Liu, L.-g. Temperature dependence of Raman spectra of the quartz- and rutile-types of GeO_2 ; *Phys. Chem. Miner.* **1997**, *24*, 7–16.
- (14) Kotsalas, I. P.; Raptis, C. High-temperature structural phase transitions of $\text{Ge}_x\text{S}_{1-x}$ alloys studied by Raman spectroscopy; *Phys. Rev. B* **2001**, *64*, 125210-1–125210-8.
- (15) Inoue, K.; Matsuda, O.; Murase, K. Raman spectra of tetrahedral vibrations in crystalline germanium dichalcogenides, GeS_2 and GeSe_2 , in high and low temperature forms; *Solid State Commun.* **1991**, *79*, 905–910.
- (16) Julien, C.; Barnier, S.; Massot, M.; Chbani, N.; Cai, X.; Loireau-Lozac'h, A. M.; Guittard, M. Raman and infrared spectroscopic studies of Ge–Ga–Ag sulphide glasses; *Mater. Sci. Eng.* **1994**, *B22*, 191–200.
- (17) Efimov, A. M. Infrared spectra, band frequencies and structure of sodium germanate glasses; *Phys. Chem. Glasses* **1999**, *40*, 199–206.
- (18) Kamitsos, E. I.; Kapoutsis, J. A.; Chrysikos, G. D.; Taillades, G.; Pradel, A.; Ribes, M. Structure and optical conductivity of silver thiogermanate glasses; *J. Solid State Chem.* **1994**, *112*, 255–261.
- (19) Lucovsky, G.; deNeufville, J. P.; Galeener, F. L. Study of the optic modes of $\text{Ge}_{0.30}\text{S}_{0.70}$ glass by infrared and Raman spectroscopy; *Phys. Rev. B* **1974**, *9*, 1591–1597.
- (20) Kawamoto, Y.; Kawashima, C. Infrared and Raman spectroscopic studies on short-range structure of vitreous GeS_2 ; *Mater. Res. Bull.* **1982**, *17*, 1511–1516.
- (21) Souquet, J. L.; Robinel, E.; Barrau, B.; Ribes, M. Glass formation and ionic conduction in the $\text{M}_2\text{S}-\text{GeS}_2$ ($\text{M} = \text{Li}, \text{Na}, \text{Ag}$) systems; *Solid State Ionics* **1981**, *3–4*, 317–321.
- (22) Popovic, Z. V.; Holtz, M.; Reimann, K.; Syassen, K. High-pressure Raman scattering and optical absorption study of $\beta\text{-GeS}_2$; *Phys. Status Solidi B* **1996**, *198*, 533–537.
- (23) Liu, X.; Tikhomirov, V.; Jha, A. Influence of vapor-phase reaction on the reduction of OH^- and S–H absorption bands in GeS_2 -based glasses for infrared optics; *J. Mater. Res.* **2000**, *15*, 2864–2874.